International Journal of Biological Macromolecules 154 (2020) 1185–1193

Contents lists available at ScienceDirect

International Journal of Biological Macromolecules

journal homepage: www.elsevier.com/locate/ijbiomac

Injectable antibacterial cellulose nanofiber/chitosan aerogel with rapid shape recovery for noncompressible hemorrhage

Xialian Fan [a], Yijin Li [b], Xiumin Li [a], Yonghui Wu [a], Keyong Tang [a,*], Jie Liu [a], Xuejing Zheng [a], Guangming Wan [c]

[a] School of Materials Science and Engineering, Zhengzhou University, Zhengzhou 450001, China
[b] The Fifth Affiliated Hospital of Zhengzhou University, Zhengzhou 450052, China
[c] The First Affiliated Hospital of Zhengzhou University, Zhengzhou 450052, China

ARTICLE INFO

Article history:
Received 29 May 2019
Received in revised form 30 October 2019
Accepted 30 October 2019
Available online 12 November 2019

Keywords:
Cellulose nanofiber
Chitosan
Aerogel
Hemostatic

ABSTRACT

Here an injectable antibacterial aerogel was fabricated with oxidized cellulose nanofiber and chitosan for rapid hemostasis of noncompressible hemorrhage application. Especially, cellulose nanofiber was modified with carboxyl groups by pre-oxidizing in 2,2,6,6-tetramethylpiperidine-1-oxyl combined with high pressure homogenization. Whereafter, the realized carboxyl group of cellulose nanofiber was reacted with the amidogen of chitosan to yield a strong composite aerogel with a nanofiber/nanosheet interlaced structure, which increased the compressive mechanical strength up to 75.4 kPa. In addition, the nanocellulose/chitosan composite aerogel exhibits high water absorption capacity, rapid shape recovery and good antibacterial ability (via *Escherichia coli* and *Staphylococcus aureus*). Once absorbing water, the nanocellulose5/chitosan5 compressed aerogel could rapidly recover its shape within 30 s. The *in vitro* coagulation ability measurement showed that the composite aerogel has a good adhesion and aggregation effect to red blood cells and platelets. Hemolysis and cytotoxicity analysis results indicated a good biocompatibility for the composite aerogel.

1. Introduction

Blood is an important carrier for transporting oxygen to the body, which will result in dysfunctional or exhaustion if too much blood is lost [1,2]. Hemorrhage is an important issue for military and civilian trauma centers worldwide, in which uncontrolled bleeding leads to more than 30% of traumatic deaths [3]. Due to the protective effect of personal protective equipment such as bulletproof vest and helmet, battlefield traumas occurs mostly in the limbs and limb joints such as armpits, groin and neck, etc. [4,5]. These parts cannot be stopped by tourniquet or artificial pressure. Moreover, the penetrating wound or deep trauma occurring in these parts is often accompanied by the rupture of the arterial blood vessels [6]. Under the action of blood pressure, the blood in human body is escaping quickly. Therefore, it is necessary to develop a hemostatic sponge which can quickly coagulate blood to form thrombosis and produce appropriate force by rapidly expansion to compress the arterial blood vessels to reduce blood loss.

Currently available hemostatic agents, such as zeolite [7], montmorillonite [8] or kaolin-based Quick Clot [9], medical gauze loaded with hemostatic drugs [10], collagen, gelatin or chitosan-based hemostatic sponges [11–13], and fibrin-based bandages [14], which have been proven to be effective in stop bleeding. However, collagen and gelatin have poor tissue adhesion, and their hemostatic function depends on sufficient platelets and clotting factors. Fibrin is derived from blood and may cause viral infection. And porous zeolite or montmorillonite powder is easy to cause wound burns or produces an inflammatory response. Some new hemostatic techniques have been invented such as XStat device (RevMedx Corporation, Oregon) [3,15–17], but the preparation of these hemostatic materials is complicated and expensive.

Abundant active hydroxyl groups on the surface of nanocellulose can be used for chemical modification, such as oxidation and polymer grafting [18]. Some recent studies have shown that 2,2,6,6-tetramethylpiperidine-1-oxyl (TEMPO) oxidized nanocellulose is beneficial to hemostasis [19], and it also shows better biocompatibility and bioactivity [20]. Chitosan has been demonstrated to be an invaluable material in the fields of biomedical engineering and biotechnology because of its wound healing effect, as well as good biocompatibility and biodegradability [21–24]. A

* Corresponding author.
E-mail address: keyongtangzzu@yahoo.com (K. Tang).

https://doi.org/10.1016/j.ijbiomac.2019.10.273
0141-8130/

mount of aerogels [25], membranes [26], gels [27] or particles [28] have been prepared based on nanocellulose for wound healing, wound hemostasis, cell culture or food packaging. Cheng et al. developed a cellulose nanocrystal/alginate composite cross-linked by Ca^{2+}, which showed good hemostatic efficiency with high tensile strength but its shape recovery ability is not mentioned [19]. Alex et al. investigated a Ca^{2+}-crosslinked nanofibrillated cellulose hydrogel as potential hemostatic wound dressing, which can be tuned to target certain wounds (e.g., strongly hemorrhaging ones) or specific phases of the wound healing process for optimal wound management [29]. Nguyen et al prepared a thermosensitive-injectable hydrogel based on TEMPO-oxidized cellulose nanofiber (TOCNF) and chitosan, which showed the addition of TOCNF could significantly improve the biocompatibility of CS hydrogel [27]. Mousumi et al. developed an oxidized cellulose (ONFC)-chitosan (Ch) sponge through lyophilization at a volume ratio of 50:50, which showed rapid hemostasis time but poor swelling ratio and mechanical strength [30]. Although these materials show excellent hemostasis properties, its poor mechanical properties and poor shape recovery make it unable to effectively seals the wound and generates appropriate force on the arterial vessels to effectively reduce arterial blood loss in face of penetrating or deep trauma [3].

For the above mentioned reasons, an injectable antibacterial cellulose nanofiber/chitosan aerogel with rapid shape recovery is prepared combing by TEMPO oxidized cellulose nanofibers and chitosan. Through TEMPO oxidation and dehydrothermal crosslinking, the composite aerogel has high water absorption capacity and mechanical properties, as well as rapid shape recovery ability which due to the carboxyl groups in the cellulose undergo condensation reaction with the amino groups of chitosan. Especially, the nanocellulose5/chitosan5 compressed aerogel can rapidly recover its shape within 30 s by absorbing water. High mechanical properties and rapid shape recovery are conducive to composite aerogel effectively seal the wound and generate appropriate force on the arterial vessels to effectively reduce arterial blood loss. Besides, the NC/CS aerogel showed good antibacterial ability against *Escherichia coli* (*E. coli*) and *Staphylococcus aureus* (*S. aureus*) which was expected to provide a sterile environment for wound healing. Dynamic whole blood clotting time was evaluated *in vitro* to investigate the blood-clotting ability of the composite aerogel. And the hemolytic activity and cytotoxicity were evaluated *in vitro* to investigate the biocompatibility of the aerogels. Hence the realized composited NC/CS aerogel was a promising rapid hemostasis material for incompressible deep trauma.

2. Experimental section

2.1. Materials

Microcrystalline cellulose (MCC) with food grade was purchased from Hubei chemical fiber factory. Chitosan (CS) with deacetylation (more than 90%) was supplied by Jinhu crust product Co., Ltd. Sodium hydroxide, hydrochloric acid, absolute ethyl alcohol and sodium hypochlorite solution (14%) with analytically pure (AR) were purchased from Tianjin Fengchuan chemical reagent technology Co., Ltd. 2,2,6,6-tetramethylpypeidine-1-oxyl (TEMPO, 99.9%, AR) and sodium bromide (99%) were obtained from Aladdin reagent (Shanghai) Co., Ltd.

2.2. Preparation of cellulose nanofiber (NC)

The oxidization method of cellulose by TEMPO/NaBr/NaClO system was referred to reported studies [28]. Briefly, the hemicellulose in MCC was removed with immersion in 10 wt% NaOH solution at 60 °C water bath for 2 h. 1.0 g obtained cellulose was uniformly dispersed in 100 mL pure water, Subsequently, TEMPO (0.1 mmol) and NaBr (1.0 mmol) were added with continuous stirring. And then 2.5 mmol sodium hypochlorite was added as oxidizing agent slowly, whose pH value was adjusted to 10 with sodium hydroxide in advance. And the mixed solution was stirred continuously for 150 min, meanwhile the solution pH maintained at about 10, at last, the reaction was terminated by ethanol and the solution was washed with deionized water until neutral. The obtained 2 wt% TEMPO oxidized cellulose (T-MCC) solution was treated by a high-pressure homogenizer, and the NC was obtained by continuous homogenizing 30 times under a pressure of 1000 bar.

3. Preparation of nanocellulose/chitosan (NC/CS) aerogels

The high viscosity chitosan was dissolved in 0.1 M acetic acid solution to obtain 1.0 wt% chitosan solution. The realized nanocellulose solution was evaporated until the concentration is 1.5 wt%. Then the nanocellulose solution and the chitosan solution were uniformly mixed at a mass ratio of 3:7, 5:5 and 7:3 at stirred at 40 °C for 4 h. The mixed solution was then poured into a mold, frozen in liquid nitrogen for 2 min, and lyophilized for 48 h successively. The freeze-dried aerogel was dry-crosslinked in a vacuum oven at 110 °C for 1 h to yield NC/CS aerogel.

3.1. Characterization

The attenuated total reflectance Fourier transform infrared spectroscopy (ATR-FTIR) was applied to measure the structure of MCC, T-MCC, CS and NC/CS aerogels with TENSOR II (Bruker, Germany) in the range of 4000–400 cm^{-1}. The cross-sectional morphologies of the NC/CS aerogels were observed by using the scanning electron microscopy (SEM, FEI Quanta 200, US).

Compression performance test of the NC and NC/CS aerogels were conducted by using a texture analyzer (TA.XT Plus, UK). Here, the freeze-dried sample was cut into cylinder with diameter of 10 mm and height of 15 mm. After fully swelling, the samples were compressed at 10 mm/min to the target strain.

4. Density, porosity and water absorption capacity of NC/CS aerogels

The sample sizes were measured according to GB/T6342-1996 file at room temperature, which were accurately measured at least three times at three different locations. And the average of each data group was used to calculate the volume and density of the NC/CS aerogels.

The porosity was obtained in a similar way as our previous work [13]. Briefly, the initial weights of aerogels were weighed as W_0, and the weight soaked sample in dehydrated alcohol for 24 h was recorded as W_t. The porosity of the aerogels were calculated according to Eq. (1):

$$P = \frac{W_t - W_0}{\rho_0 V_0} \times 100\% \quad (1)$$

where P is the porosity, W_0 is the initial weight of the aerogel, W_t is the weight of the swollen aerogel, V_0 is the initial volume of the aerogel, and ρ_0 is the density of dehydrated alcohol (0.79 g/mL).

The water absorption ability of NC and NC/CS aerogels were studied by immersing the aerogels in 50 mL water adequately. Then the immersed aerogels were taken out and hold it for a while until no water dropping. Herein the immersed aerogel was weighed again. And the water absorption capacity (g/g) of aerogels were measured and calculated according to Eq. (2):

$$Water\ absorption\ capacity = \frac{w_2 - w_1}{w_1} \quad (2)$$

where w_2 and w_1 are weights of fully water saturated and dry aerogels, respectively.

4.1. Blood cells adhesion

Whole blood cells adhesion was conducted referring to the published literature [19]. In brief, the NC/CS aerogels were cut into cylindrical aerogels with a height of 10 mm and a diameter of 10 mm, and then immersed in PBS (pH = 7.4) at 37 °C for 1 h. Subsequently, the whole blood was added dropwise into the aerogels and incubated at 37 °C for 5 min. All the aerogels were then washed with PBS solution three times to remove the physical adhered blood cells, and then the adhered blood cells were fixed by 2.5% glutaraldehyde for another 2 h. After that, the bloods cells were dehydrated with 50%, 60%, 70%, 80%, 90% and 100% ethanol solution with the interval of 10 mins, respectively. The dried samples were observed using SEM.

4.2. Whole-blood clotting

The whole-blood clotting of the aerogels were tested according to the reported literature [3]. The aerogels were cut into cylindrical aerogels with a height of 10 mm and a diameter of 10 mm. 50 μL recalcified whole-blood solution (0.2 M $CaCl_2$, 10 mM in the blood) was added on the aerogels (the aerogels were preheated at 37 °C for 5 min) in polypropylene tubes, respectively. The tube was then incubated at 37 °C for 30 s, 60 s, 90 s, 120 s and 150 s, respectively. The gauze and gelatin hemostatic sponge were used as references. After incubation, 10 mL deionized water was gently added to release unbound blood without disturbing the clot. The absorbance of the supernatant was recorded at 540 nm by using a spectrophotometer (Multiskan GO, Finland). The absorbance of 50 μL of recalcified whole-blood in 10 mL deionized water was used as the negative reference. The blood clotting index (BCI) was calculated by using Eq. (3):

$$BCI(\%) = \frac{I_s - I_0}{I_r - I_0} \times 100\% \quad (3)$$

where I_s represents the absorbance of sample and I_r represents the absorbance of the negative control.

4.3. Antibacterial activity

Staphylococcus aureus (*S. aureus*) and Escherichia coli (*E. coli*) bacteria liquids were prepared according to our previous study [13]. The aerogels were cut into disks with a height of 2 mm and diameter of 5 mm, and fully sterilization under 254 nm UV irradiation for 30 min. A gar medium was prepared and the bacteria liquids was coated on the solid medium. A round hole with 5 mm diameter was made on the solid medium with a perforator, and the aerogel sample was gently placed into the round hole and continuously cultured at 37 °C for 24 h. Then the petri dish was taken out and photographed with a digital camera.

4.4. Hemolytic activity assay in vitro

The hemolytic activity assay *in vitro* of the aerogels were tested according to the literature [3]. Briefly, fresh blood from human was put into centrifuge tube and centrifuged (1000 rpm) at room temperature for 10 min. Washing with sterile saline centrifuging until the supernatant was clear, the supernatant fluid was wiped after the last centrifugation and the erythrocytes at the bottom were obtained, and the erythrocytes with the concentration of 5% (v/v) were diluted with sterile saline for subsequent use. The Freeze-dried aerogel was then smashed into homogenate and four aerogel dispersion liquids (with the concentrations of 0.5 mg/mL, 1 mg/mL, 2 mg/mL and 5 mg/mL) were prepared. 0.5 mL aerogel dispersion liquid and 500 μL of erythrocyte suspension (5% (v/v)) were added into a 2-mL tube, and evenly mixed. After placed at 37 °C for 1 h, all the samples were centrifuged (1000 rpm) for 10 min. The absorbance of the supernatant was recorded at 540 nm by using a spectrophotometer (Multiskan GO, Finland). Three to five replicates were performed. Deionized water was as positive group and sterile saline was as negative group. The hemolysis ratio of the aerogel was calculated using the Eq. (4):

$$Hemolysis\ (\%) = \frac{A_p - A_b}{A_t - A_b} \times 100\% \quad (4)$$

where A_p is the absorbance of the aerogels, A_t is the absorbance of the positive group and A_b is the absorbance of the negative group.

4.5. Cytotoxicity test

The cytotoxicity of the NC, NC7/CS3, NC5/CS5 and NC3/CS7 aerogels were determined by a MTT colorimetric method, performed in a similar way to our previous work [13,31]. Briefly, 10% DMEM medium containing 10% calf serum was added to the scaffolds at the proportion of 0.1 g/mL, and cultured at 37 °C and 50% relative humidity for 24 h. The mouse fibroblasts (Fbs) were cultured with the leaching solution of the samples, and the control was cultured with 10% DMEM medium containing 10% calf serum. 10^5/mL cell suspension was prepared with the 5–10 generations of Fbs cells, followed by a continuous culture for 1 day and 3 days. The culture solution was changed every two days. Each hole was added with 20 μL 5 mg/mL MTT and continuously cultured for 4 h. The medium was replaced with 200 μL dimethyl sulfoxide (DMSO), and the plate was shocked for 10 min. The absorbance (Abs) was analyzed by using a spectrophotometer (Multiskan GO, Finland) at 570 nm, and five parallel experiments of each sample were done with the averages reported. The relative growth rates (RGR) were calculated according to Eq. (5):

$$E = \frac{A_1}{A_0} \quad (5)$$

where E is the RGR, A_1 is the Abs of experimental, and A_0 is the Abs of blank. The cytotoxicity of porous scaffolds according to ISO/TC194 file.

5. Results and discussion

The high water absorption and rapid shape recovery of cellulose aerogel make it a promising application in rapid hemostasis. Due to the great amount of hydrogen bond on the molecular chain of cellulose, the cellulose fibers are entangled with each other to form a fiber bundle with a diameter about 10 μm, making them difficult to be mixed uniformly in the solution to prepare cellulose aerogels with good structure and performance. Physical or chemical methods were usually used to process cellulose fiber bundles to achieve nanoscale and increase the dispersion of cellulose. As shown in Fig. 1a, the cellulose was modified by TEMPO/NaBr/NaClO, which selectively oxidized the primary hydroxyl group on the C6 in the cellulose glucose unit to carboxyl group, and destroyed the inside hydrogen bond structure of the cellulose. From the infrared spectrum in Fig. S1 of supplementary data, it should be noted that the T-MCC exhibits C═O characteristic absorption peak at 1725 cm^{-1}, and —CO— stretching vibration characteristic absorption peak near 1320 cm^{-1}, indicating the formation of carboxyl group is on the molecular chain of cellulose. The carboxyl content

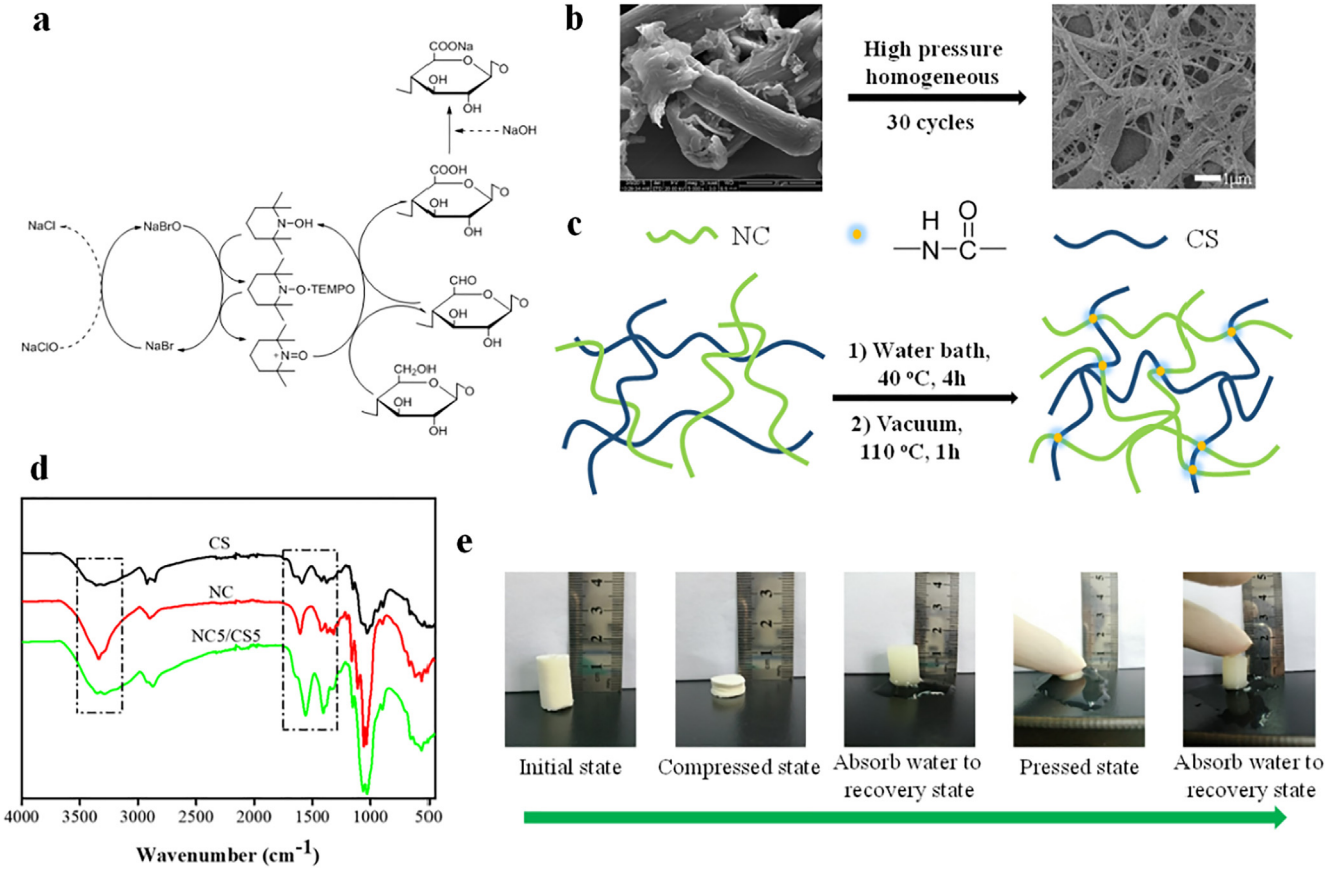

Fig. 1. (a) Preparation of T-MCC using TEMPO/NaBr/NaClO, (b) NC with a size about 100 nm by T-MCC with high pressure homogenization, (c) schematic diagram of preparation of NC/CS composite aerogel, (d) FT-IR spectra of CS, NC and NC5/CS5 aerogels, (e) absorbing water to recovery of NC5/CS5 aerogel under different shapes.

of cellulose-MCC was determined by conductometric titration with the results shown in Fig. S2 of supplementary data. The carboxyl content of cellulose increases with increasing the amount of NaClO, and the carboxyl content is 6.1 mmol/g cellulose when the amount of NaClO is 2.5 mmol. With the shearing action of high-pressure homogenizer, the cellulose size is transformed from microscale to nanoscale (Fig. 1b). From the transmission electron micrograph images in Fig. S3 of supplementary data, the cellulose nanofibers exhibit better uniformly distributed network structure compared to the unoxidized cellulose nanofibers, and richer network with increasing the NaClO amount. The size of nanocellulose is about 100 nm, indicating that higher oxidation degree of cellulose is beneficial to the microfibrillation of cellulose in high pressure homogenization. During the oxidation process, TEMPO selectively oxidizes the primary hydroxyl group on C6 in the cellulose glucose unit and destroys partial hydrogen bonds between molecules. Single fibrils are more easily getting rid of the hydrogen bonds to form more uniform fiber network under high pressure homogenization.

The nanocellulose/chitosan composite aerogels are prepared by mixing the oxidized nanocellulose with chitosan (Fig. 1c), the amide condensation reaction taking place between the carboxyl group on nanocellulose and the amino group on chitosan, which is conducive to improve the structural stability of NC/CS aerogel. The peaks around 3283 cm^{-1} and 1560 cm^{-1} are attributable to N-H stretching vibration absorption, and the peaks near 1657 cm^{-1} and 1318 cm^{-1} are due to C-N stretching, which suggests the formation of amide bond between nanocellulose and chitosan (Fig. 1d). Pure oxidized nanofiber aerogel is easily broken under press, while the NC5/CS5 aerogel with 50 wt% content chitosan can withstand hundreds of repeated press and still maintain the shape stability. The introduction of chitosan can better improve the structural stability of the cellulose aerogel. As shown in Fig. 1e, the freeze-dried NC5/CS5 composite aerogel is squeezed to a certain shape, and it can quickly recover to the original shape with absorbing water. The aerogel is still able to quickly absorb water to recover to its original shape when the water is repeatedly squeezed out from the aerogel. Through TEMPO oxidation and dehydrothermal treatment, the composite aerogel behaves good structural stability.

The scanning electron micrographs of the MCC, MFC, T-MFC, NC7/CS, NC5/CS5 and NC3/CS7 aerogels are showed in Fig. 2. It can be found that the MCC is rod-shaped fiber with a diameter of about 10 μm, while the MCC without oxidized by TEMPO/NaBr/NaClO is microfibrillated to form fiber network (MFC) with a diameter of 500 nm under high pressure homogenization, but the fibers are closely entangled. And the MCC oxidized by TEMPO/NaBr/NaClO is microfibrillated to form uniform fiber network structure with a diameter of 100 nm under high pressure homogenization, and the oxidation of cellulose can improve the degree of cellulose shear in the process of high pressure homogenization. (Fig. 3S in supplementary data). The T-MFC showed a better uniform network structure and the fiber diameter was about 100 nm. The aerogel mainly showed fibrous reticular structure when the content of chitosan was 30%, and the structure of aerogels changed from reticular to lamellar with the increasing content of chitosan. NC5/CS5 showed the coexistence of fibrous reticular and lamellar structure. The composite aerogel exhibits a sheet structure when the chitosan content is up to 70%. Both fiber network and sheet structure exist in the aerogel, which is conducive to improve mechanical strength and water absorption capacity, and the introduction of

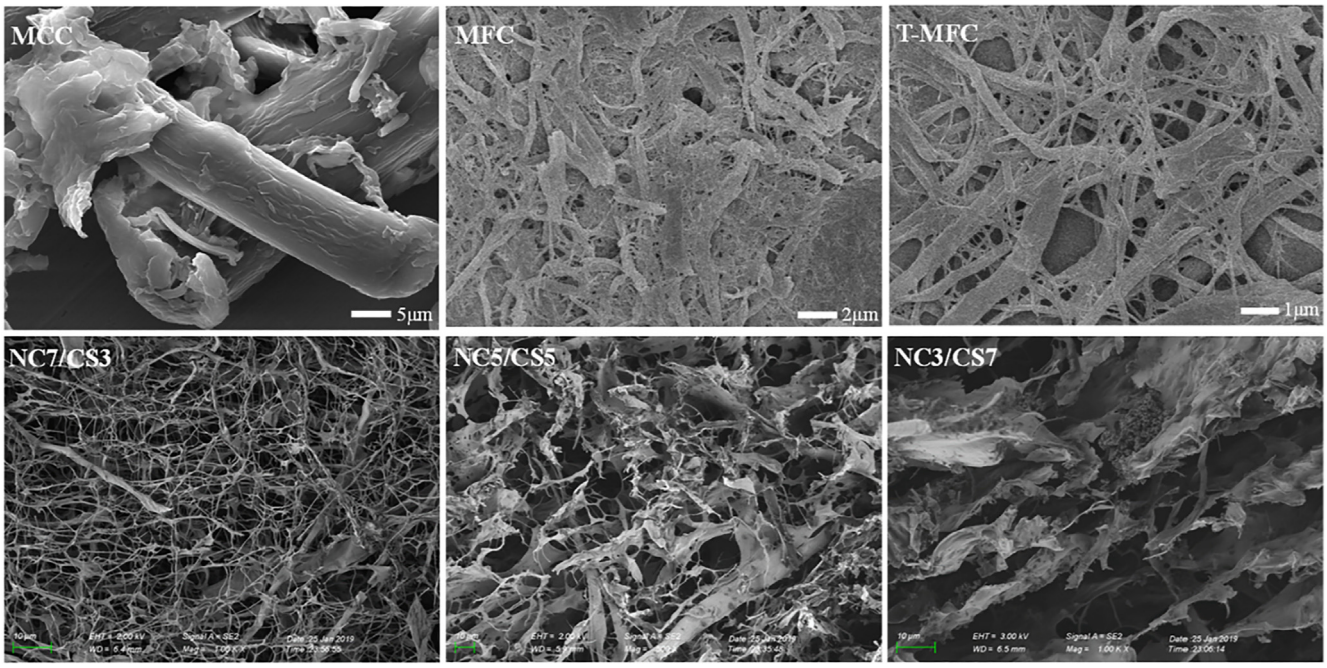

Fig. 2. SEM micrographs of the MCC, MFC and T-MFC, and the cross section of NC7/CS3, NC5/CS5 and NC3/CS7 aerogel.

chitosan helps to increase the structural stability of the cellulose aerogel.

The density, porosity, water absorption and compression strength of the composite aerogel were showed in Fig. 3. The density and porosity of NC aerogels were 14.3 mg/cm^3 and 97.5%, respectively. With increasing the chitosan content, the density of NC7/CS3, NC5/CS5 and NC3/CS7 gradually increases, 18.7 mg/cm^3, 21.7 mg/cm^3, and 26.5 mg/cm^3, respectively. Nevertheless, the porosity of the corresponding aerogels gradually decreases, 93.3%, 91.2%, and 87.1%, respectively. It can also be seen from the scanning electron microscope images of NC7/CS3, NC5/CS5 and NC3/CS7, the composite aerogels gradually changing from a porous network structure to a sheet structure with increasing the chitosan content. The water absorption capacity of the aerogels is essential for condensing blood and quickly stopping bleeding, and the aerogel with high water absorption capacity can quickly absorb water in the blood to achieve rapid coagulation. As shown in Fig. 3c, the water absorption capacities of NC, NC7/CS3, NC5/CS5 and

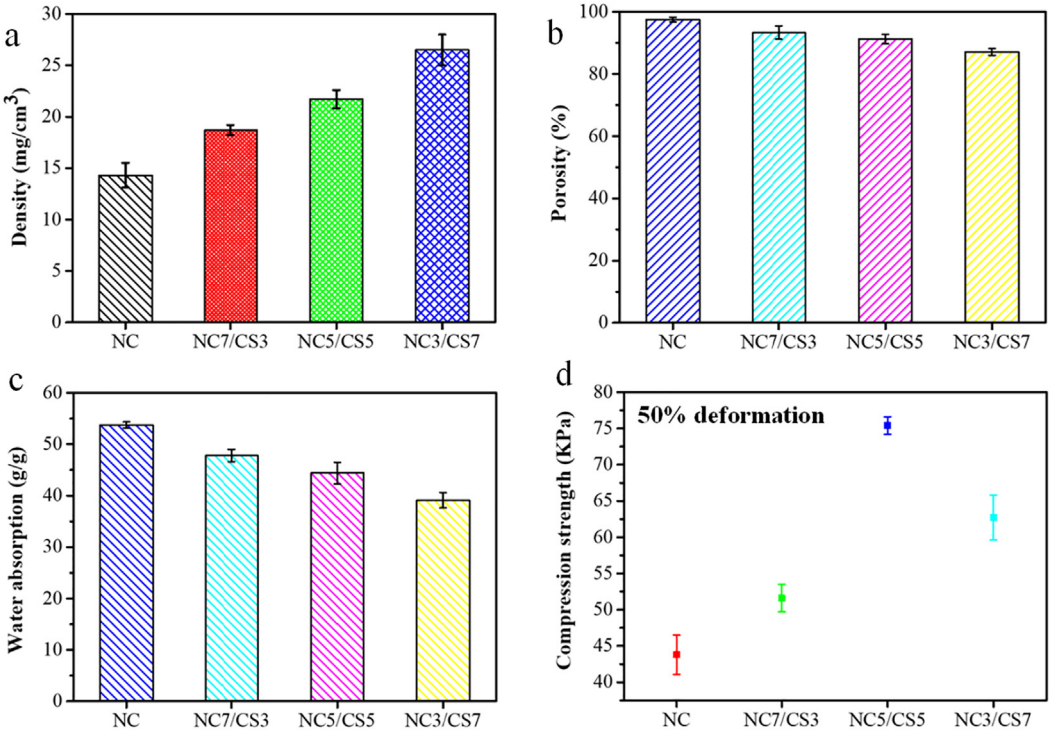

Fig. 3. Density, porosity, water absorption and compression strength (50% deformation) of NC, NC7/CS3, NC5/CS5 and NC3/CS7 aerogels.

NC3/CS7 are 53.7 g/g, 47.8 g/g, 44.4 g/g and 39.1 g/g, respectively, and the water absorption capacity of the aerogels gradually decreases with increasing the chitosan content. The nanocellulose contains a large number of hydrophilic groups and a rich pore network structure in pure nanocellulose aerogel, which help pure nanocellulose aerogel absorb more water. With increasing the chitosan content, the nanocellulose content decreases and the structure of composite aerogel changes from porous fiber to lamellar layer, which is not conducive to the water absorption of composite aerogel. High water absorption capacity and mechanical properties are beneficial to quickly absorb the water in the blood and concentrate the blood to form thrombus so as to promote hemostasis.

Deep wounds are often accompanied by rupture of arterial blood vessels. The human arterial blood pressure is about 12–15 kPa. Without external force, blood in arterial blood vessels will be quickly lost from the body by spraying. Therefore, it is necessary to use external force to press the arterial blood vessels to reduce blood loss. For noncompressible wounds, tourniquets or artificial pressure are not effective in applying an appropriate force on the wound. In this case, sufficient force is needed to be exerted by the hemostatic material itself. As can be seen from Fig. 3d, the compression strength of NC, NC7/ The CS3, NC5/CS5 and NC3/CS7 aerogels at the deformation of 50% is 43.8 kPa, 51.6 kPa, 75.4 kPa and 62.7 kPa, respectively. The expanded aerogel can produce enough force to compress the arterial vessels to reduce the loss of arterial blood, which is conducive to stop bleeding.

Fig. 4 shows the antibacterial ability of the composite aerogel against *E. coli* and *S. aureus*. Pure NC aerogel has no antibacterial effect on *E. coli* and *S. aureus*. With the addition of chitosan, the composite aerogels show better antibacterial effect, and the antibacterial effect increases with increasing the chitosan content. Under the external forces, many bacteria might be brought into the deep wound or through and through wound, and these bacteria are not easily washed out by traditional disinfectant. The NC/CS composite aerogel has good antibacterial effect which can inhibit the growth of bacteria inside the wound and provide a clean environment. Especially in the battlefield or major accident, it may efficiently reduce the chance of wound infection and increase the survival rate of the wounds.

The coagulation ability of the aerogel was evaluated by dynamic whole blood clotting time detection, the higher absorbance of the hemoglobin solution and the slower blood agglutination rate of the aerogels. Traditional hemostatic reagent gauze and gelatin sponge as the control. It can be clearly seen from Fig. 5a that the absorbance of hemoglobin solution of nanocellulose aerogel at different time points is lower than that of gauze and gelatin sponge, indicating that the nanocellulose aerogel has better coagulation ability. The high water absorption capacity of nanocellulose aerogel can quickly absorb the water in the blood and accumulate red blood cells and platelets to achieve hemostasis. After the introduction of chitosan, NC7/CS3, NC5/CS5 and NC3/CS7 showed better coagulation ability compared to NC, especially NC5/CS5. It might be that the positive charge on the surface of the chitosan reacts with the negative charge on the surface of the red blood cell, causing the red blood cells to adhere and form a blood clot, thereby coagulating the blood.

The hemostatic mechanism of aerogels is further investigated by observing the adhesion state and morphological distribution of blood cells on the surface of the aerogel. It can be clearly seen from the scanning electron micrograph that a large number of blood cells adhere to the surface of NC7/CS3, NC5/CS5 and NC3/CS7 aerogels, and the blood cells exhibit an irregular aggregate structure (Fig. 5b). The blood cells on the surface of NC7/CS3 and NC5/CS5 aerogels were significantly more than those of the NC3/CS7 group, which might be the fibrous reticular is conducive to cell adhesion and aggregation. The nanocellulose aerogels absorb water from the blood to concentrate the blood cells between the fiber networks, making it easy for blood cells to form a clot and stop bleeding. The aerogel with interconnected porous and high water absorption capacity could absorb water quickly from the blood and form a clot that blocks the blood vessels bleeding, and exhibit better *in vitro* coagulation ability. The good adhesion and aggregation ability of aerogel to blood cells and the rapid whole blood coagulation rate can improve the hemostatic rate of aerogel used in penetrating or deep wound wounds.

Currently, the most common method of closing deep wounds is to fill the wound with gauze to apply pressure on the wound to reduce blood loss. However, the method is limited, and the possibility of death for the wounded is still not little. Fig. 6a shows the simulation of injecting compressed composite aerogels into wound. The composite aerogels are compressed into sheet, placed into syringe and squeezed into the wound. The compressed aerogels can absorb the blood and rapidly expand to fully fill the wound. At the same time, the expanded aerogel can exert pressure on the arterial blood vessels to reduce the re-flow of arterial blood. Fig. 6b shows the shape change of the NC5/CS5 compressed aerogel in water over time. The NC5/CS5 compressed aerogel can absorb water with rapid deformation recovery within 30 s, and the process of rapid shape recovery of the aerogel may be seen in the video of supplementary data. The fast deformation recovery property of aerogels is conducive to use in incompressible deep wounds. Meanwhile, the rapid expansion of the volume of the composite aerogel can seal the wound, which is beneficial to reduce the entry of bacteria and reduce wound infection.

Hemolysis test *in vitro* is a general method to evaluate the blood compatibility of biomaterials. The hemolysis of aerogels *in vitro* was tested with different concentrations of aerogel extracts (500 μg/mL, 1000 μg/mL, 2000 μg/mL, 5000 μg/mL). The macro-

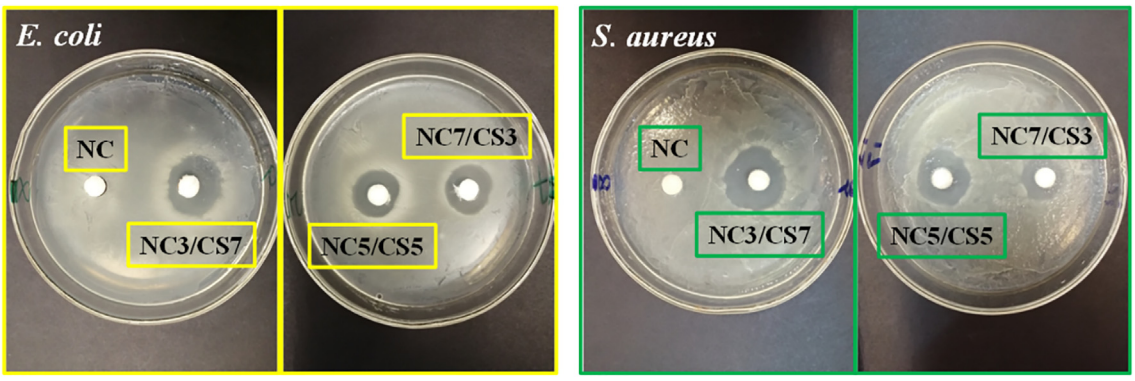

Fig. 4. Antibacterial ability of NC, NC7/CS3, NC5/CS5 and NC3/CS7 aerogels against *E. coli* and *S. aureus*.

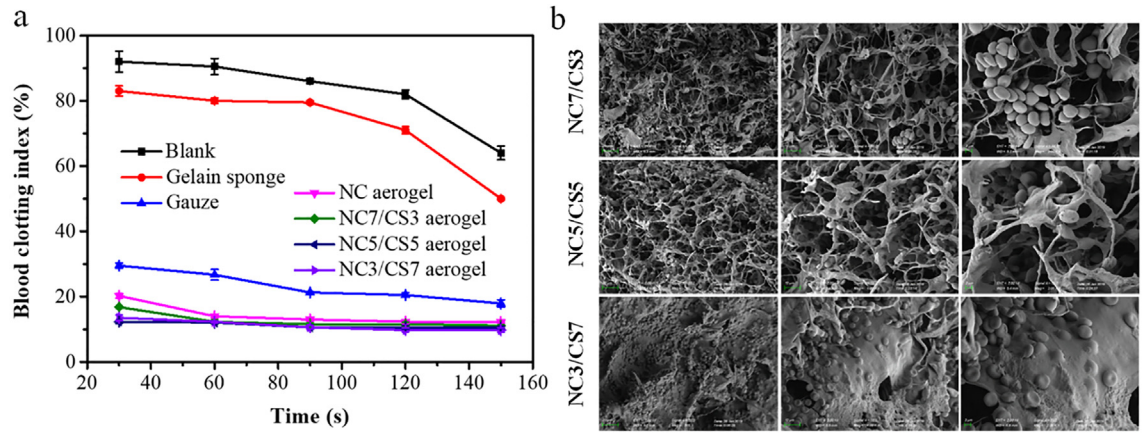

Fig. 5. (a) *In vitro* dynamic whole blood clotting evaluation of the NC, NC7/CS3, NC5/CS5 and NC3/CS7 aerogels, gelatin sponge and gauze as the control, (b) SEM images of blood cells adhesion on the NC, NC7/CS3, NC5/CS5 and NC3/CS7 aerogels.

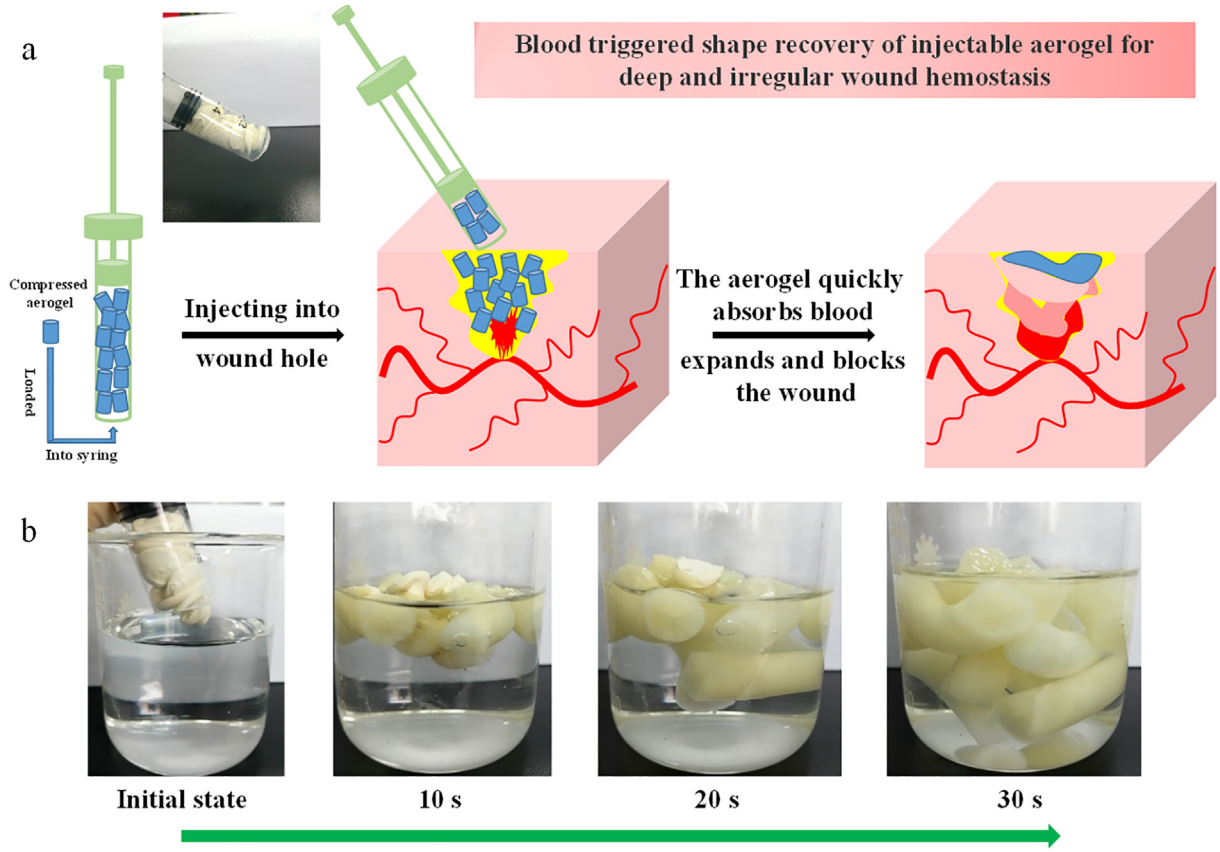

Fig. 6. (a) Schematic diagram of the process of simulating the injection of composite aerogel into the wound, (b) digital photos of NC5/CS5 aerogel with rapid shape recovery after water absorption.

scopic photographs of the centrifuged supernatants of the four groups of aerogels, positive and negative groups are shown in Fig. 7a, and the four groups of aerogels were all reddish, similar to the negative group, and the positive group was bright red. The specific values of the hemolysis rate of the four groups of aerogels are shown in Fig. 7b. NC5/CS5 showed lower hemolysis rate, compared with the other three groups. When the concentration of the extract was 5000 μg/mL, the hemolysis rates of NC5/CS5 and NC3/CS7 were both about 1.59%, while those of NC7/CS3 and NC were 2.3% and 2.7%, respectively, indicating better biocompatibility for NC5/CS5 and NC3/CS7. Although aerogels exhibit different hemolysis rates, they have better biocompatibility than previously reported (7.1%) hemostatic materials [25,31]. These hemolysis structures indicate good blood compatibility for aerogels as rapid hemostatic materials.

The relative cell proliferation rate of the four aerogels are shown in Fig. 7c. On day 1, the relative cell proliferation rates of NC, NC7/CS3, NC5/CS5 and NC5/CS5 were 83.3%, 99.6%, 97.3% and 104.9%, respectively. Further cultured for 3 days, the relative cell proliferation rates were 84.1%, 91.2%, 88.3% and 97%, slightly lower than that in 1 day. However, with reference to the cytotoxicity level, all four aerogel materials were above grade I, meaning no

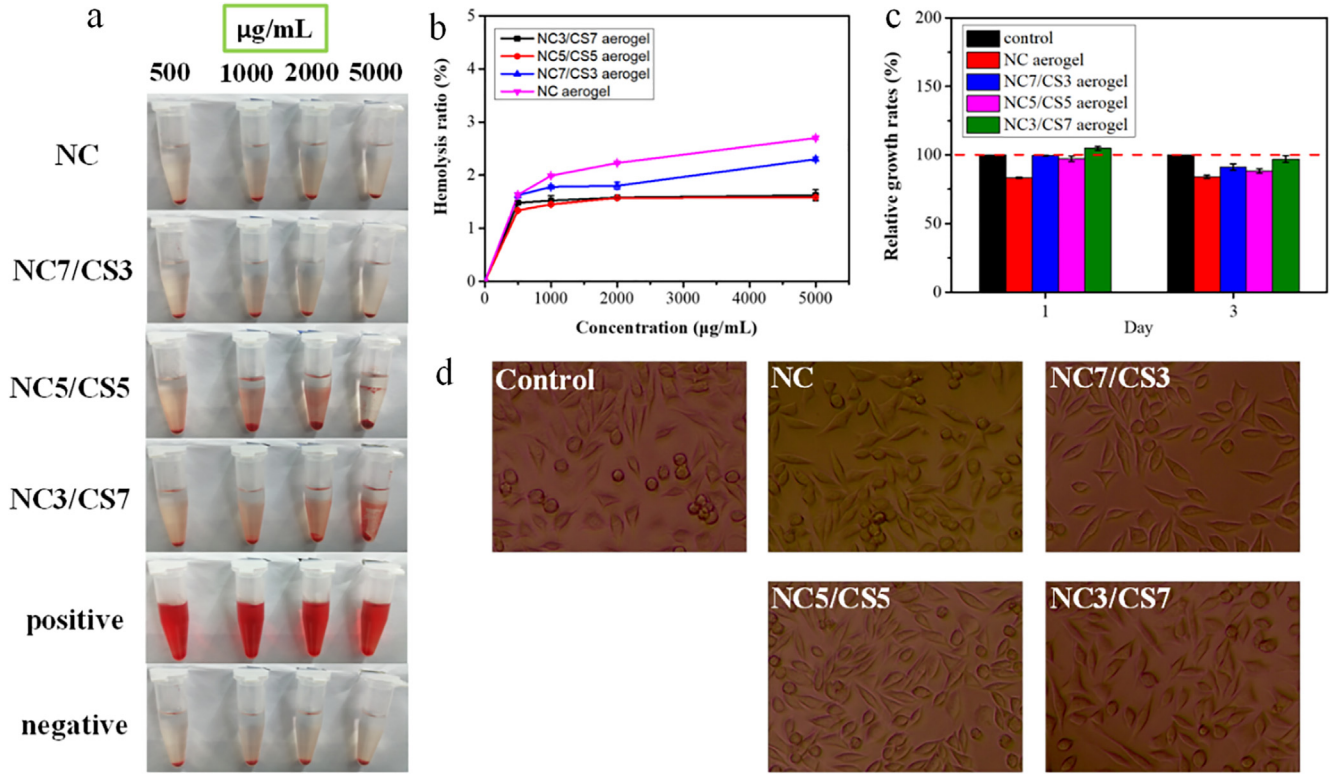

Fig. 7. (a) Photographs from hemolytic activity assay of the NC, NC7/CS3, NC5/CS5 and NC3/CS7 aerogels using sterile saline as negative control and deionized water as positive control, (b) hemolytic ratio of NC, NC7/CS3, NC5/CS5 and NC3/CS7 aerogels dispersion liquids at different concentrations, (c) relative growth ratios of the NC, NC7/CS3, NC5/CS5 and NC3/CS7 aerogels after 1 and 3 days, (d) optical microscopy of cell morphology of fibroblasts grown in aerogel extract for 3 days.

cytotoxicity. The growth state of fibroblasts continuously cultured for 3 days are shown in Fig. 7d. Compared with the negative group, the fibroblasts of the experimental group showed good growth state, and the composite aerogel might satisfy the requirement of good biocompatibility of fast hemostatic biomaterial.

6. Conclusion

In this work, nanocellulose fibers with uniform dispersion and average size of about 100 nm were prepared by the combination of TEMPO oxidation and high-pressure homogenization. And the nanocellulose/chitosan composite aerogels with high water absorption capacity and rapid shape recovery are successfully obtained by combing cellulose nanofiber with chitosan. The introduction of chitosan can not only improve the mechanical properties of nanocellulose aerogel, but it also significantly enhance its antibacterial effect. Through amide condensation and dehydrothermal crosslinking, the composite nanocellulose/chitosan aerogel behaves good mechanical strength up to 75.4 kPa and structural stability. Especially, the NC5/CS5 aerogel a nanofiber/-nanosheet interlaced structure can maintain structural stability without damaged undergoes several hundreds of repeated compression with increasing the content of chitosan to 50 wt%. And the NC5/CS5 compressed aerogel can rapidly recover shape within 30 s by absorbing water. Meanwhile, the antibacterial ability and *in vitro* coagulation ability of the composite aerogel increases with increasing the content of chitosan. Injecting composite aerogel to penetrating wound or deep trauma wound, compressed composite aerogel can quickly absorb blood and promote the formation of thrombosis. Furthermore, the expansion of the compressed aerogels quickly seal the wound to resist outside bacteria to enter and reduce the risk of wound infection, and the expanded aerogels can produce enough force to compress the arterial vessels to reduce the loss of arterial blood. Hence, the realized nanocellulose/chitosan composite aerogel with good biocompatibility shows promising application potential for noncompressible hemorrhage.

Acknowledgment

The financial support of this work by the National Natural Science Foundation of China (Grant No. 51673177 51373158) and the Sci-Tech. Innovation Talent Foundation of Henan Province (No. 144200510018) is gratefully acknowledged.

Appendix A. Supplementary material

Supplementary data to this article can be found online at https://doi.org/10.1016/j.ijbiomac.2019.10.273.

References

[1] Y. Jia, L. Duan, J. Li, Hemoglobin-based nanoarchitectonic assemblies as oxygen carriers, Adv. Mater. 28 (2016) 1312–1318.
[2] N.J. Abbott, A.A.K. Patabendige, D.E.M. Dolman, S.R. Yusof, D.J. Begley, Structure and function of the blood–brain barrier, Neurobiol. Dis. 37 (2010) 13–25.
[3] X. Zhao, B. Guo, H. Wu, Y. Liang, P.X. Ma, Injectable antibacterial conductive nanocomposite cryogels with rapid shape recovery for noncompressible hemorrhage and wound healing, Nat. Commun. 9 (2018) 2784.
[4] H.B. Alam, D. Burris, J.A. DaCorta, P. Rhee, Hemorrhage control in the battlefield: role of new hemostatic agents, Mil. Med. 170 (2005) 63–69.
[5] L. Mathieu, F. Bazile, R. Barthélémy, P. Duhamel, S. Rigal, Damage control orthopaedics in the context of battlefield injuries: the use of temporary external fixation on combat trauma soldiers, Orthop. Traumatol.-Sur 97 (2011) 852–859.
[6] R.B. Bell, T. Osborn, E.J. Dierks, B.E. Potter, W.B. Long, Management of penetrating neck injuries: a new paradigm for civilian trauma, J. Oral Maxil. Surg. 65 (2007) 691–705.
[7] J.W. Carraway, D. Kent, K. Young, A. Cole, R. Friedman, K.R. Ward, Comparison of a new mineral based hemostatic agent to a commercially available granular zeolite agent for hemostasis in a swine model of lethal extremity arterial hemorrhage, Resuscitation 78 (2008) 230–235.

[8] G. Li, K. Quan, Y. Liang, T. Li, Q. Yuan, L. Tao, X. Wang, Graphene-montmorillonite composite sponge for safe and effective hemostasis, ACS Appl. Mater. Inter. 8 (2016) 35071–35080.
[9] D. Trabattoni, P. Gatto, A.L. Bartorelli, A new kaolin-based hemostatic bandage use after coronary diagnostic and interventional procedures, Int. J. Cardiol. 156 (2012) 53–54.
[10] L.F. Littlejohn, J.J. Devlin, S.S. Kircher, R. Lueken, M.R. Melia, A.S. Johnson, Comparison of Celox-A, ChitoFlex, WoundStat, and combat gauze hemostatic agents versus standard gauze dressing in control of hemorrhage in a swine model of penetrating trauma, Acad. Emerg. Med. 18 (2011) 340–350.
[11] A.M. Behrens, M.J. Sikorski, P. Kofinas, Hemostatic strategies for traumatic and surgical bleeding, J. Biomed. Mater. Res. A. 102 (2014) 4182–4194.
[12] G. Lan, B. Lu, T. Wang, L. Wang, J. Chen, K. Yu, D. Wu, Chitosan/gelatin composite sponge is an absorbable surgical hemostatic agent, Colloid. Surface. B 136 (2015) 1026–1034.
[13] X.L. Fan, K.K. Chen, X.C. He, N. Li, J.B. Huang, K.Y. Tang, F. Wang, Nano-TiO_2/collagen-chitosan porous scaffold for wound repairing, Int. J. Biol. Macromol. 91 (2016) 15–22.
[14] S. Seetharaman, S. Natesan, R.S. Stowers, C. Mullens, D.G. Baer, L.J. Suggs, R.J. Christy, A PEGylated fibrin-based wound dressing with antimicrobial and angiogenic activity, Acta Biomater. 7 (2011) 2787–2796.
[15] T.L. Landsman, T. Touchet, S.M. Hasan, C. Smith, B. Russell, J. Rivera, E. Cosgriff-Hernandez, A shape memory foam composite with enhanced fluid uptake and bactericidal properties as a hemostatic agent, Acta Biomater. 47 (2017) 91–99.
[16] Y. Wang, C. Wang, L. Qiao, J. Feng, Y. Zheng, Y. Chao, M. Li, Shape-adaptive composite foams with high expansion and absorption used for massive hemorrhage control and irregular wound treatment, Appl. Mater. Today 13 (2018) 228–241.
[17] Y. Zhang, J. Guan, J. Wu, S. Ding, J. Yang, J. Zhang, L. Deng, N-alkylated chitosan/graphene oxide porous sponge for rapid and effective hemostasis in emergency situations, Carbohyd. Polym. 219 (2019) 405–413.
[18] N. Lin, J. Huang, P.R. Chang, J. Feng, J. Yu, Surface acetylation of cellulose nanocrystal and its reinforcing function in poly (lactic acid), Carbohyd. Polym. 83 (2011) 1834–1842.
[19] F. Cheng, C. Liu, X. Wei, T. Yan, H. Li, J. He, Y. Huang, Preparation and characterization of 2, 2, 6, 6-tetramethylpiperidine-1-oxyl (TEMPO)-oxidized cellulose nanocrystal/alginate biodegradable composite dressing for hemostasis applications, ACS Sustain. Chem. Eng. 5 (2017) 3819–3828.
[20] A. Shimotoyodome, J. Suzuki, Y. Kumamoto, T. Hase, A. Isogai, Regulation of postprandial blood metabolic variables by TEMPO-oxidized cellulose nanofibers, Biomacromolecules 12 (2011) 3812–3818.
[21] I. Hamed, F. Özogul, J.M. Regenstein, Industrial applications of crustacean by-products (chitin, chitosan, and chitooligosaccharides): A review, Trends Food Sci. Tech. 48 (2016) 40–50.
[22] W. Suginta, P. Khunkaewla, A. Schulte, Electrochemical biosensor applications of polysaccharides chitin and chitosan, Chem. Rev. 113 (2013) 5458–5479.
[23] B.K. Gu, S.J. Park, M.S. Kim, C.M. Kang, J.I. Kim, C.H. Kim, Fabrication of sonicated chitosan nanofiber mat with enlarged porosity for use as hemostatic materials, Carbohyd. Polym. 97 (2013) 65–73.
[24] Z. Hu, D.Y. Zhang, S.T. Lu, P.W. Li, S.D. Li, Chitosan-based composite materials for prospective hemostatic applications, Mar. Drugs 16 (2018) 273.
[25] T. Lu, Q. Li, W. Chen, H. Yu, Composite aerogels based on dialdehyde nanocellulose and collagen for potential applications as wound dressing and tissue engineering scaffold, Compos. Sci. Technol. 94 (2014) 132–138.
[26] S. Taokaew, S. Seetabhawang, P. Siripong, M. Phisalaphong, Biosynthesis and characterization of nanocellulose-gelatin films, Materials 6 (2013) 782–794.
[27] T.H.M. Nguyen, C. Abueva, H. Van Ho, S.Y. Lee, B.T. Lee, *In vitro* and *in vivo* acute response towards injectable thermosensitive chitosan/TEMPO-oxidized cellulose nanofiber hydrogel, Carbohyd. Polym. 180 (2018) 246–255.
[28] E.A. Hassan, M.L. Hassan, R.E. Abou-Zeid, N.A. El-Wakil, Novel nanofibrillated cellulose/chitosan nanoparticles nanocomposites films and their use for paper coating, Ind. Crop. Prod. 93 (2016) 219–226.
[29] A. Basu, J. Hong, N. Ferraz, Hemocompatibility of Ca^{2+}-Crosslinked Nanocellulose Hydrogels: Toward Efficient Management of Hemostasis, Macromol. Biosci. 17 (2017) 1700236.
[30] M. Sukul, R.D. Ventura, S.H. Bae, H.J. Choi, S.Y. Lee, B.T. Lee, Plant-derived oxidized nanofibrillar cellulose-chitosan composite as an absorbable hemostat, Mater. Lett. 197 (2017) 150–155.
[31] X.C. He, X.L. Fan, W.P. Feng, Y. Chen, T. Guo, F. Wang, K.Y. Tang, Incorporation of microfibrillated cellulose into collagen-hydroxyapatite scaffold for bone tissue engineering, Int. J. Biol. Macromol. 115 (2018) 385–392.